

Using unmixing methods to classify lithological and alteration units based on hyperspectral images

Saeed Goodarzi Mehr^{1,*}, Seyyed Kazem Alavipanah¹, Ali Darvishi Bloorani¹, Bahram Bahrambeigi²

1- Department of Cartography, Faculty of Geography, University of Tehran, Tehran, Iran.

2- Department of Geology, Shahid Bahonar University, Kerman, Iran.

* Corresponding Author: goodarzi.saeed@ut.ac.ir

Received: 2 November 2013 / Accepted: 6 March 2013 / Published online: 10 March 2013

Abstract

Nowadays providing geologic maps using satellite images has been developed. By using hyperspectral images more accurate studies in a wide range have been done. Since it is so expensive to provide these maps with field measurements therefore it is better to use new methods. This study provides a lithological and alteration mapping units with dominant minerals based on hyperspectral images of EO1-Hyperion satellite. To do so, two different zones were investigated: the Cuprite-Nevada and Mozahem volcano in Iran which have suitable conditions for our study. Five methods with different structures have been used: SAM, ACE, CEM, OSP, and LSU to evaluate their ability of geological unit separation. The results show that the differences and separability level in spectral signatures of training data are main factors in affecting the results in covariance base methods but it is low in the linear methods. This study revealed the accuracy of 86.45% for LSU in mineral mapping of Cuprite area and 69.54% for ACE in alteration mapping for Mozahem volcano which displays more efficiency than the other methods.

Keywords: Hyperspectral Remote Sensing, Unmixing, MNF, Mineral mapping, Alteration mapping.

1- Introduction

Since high ability of hyperspectral images in identifying geological features, this technique of remote sensing has been increased in recent years (Vane et al, 1985, Vane and Goetz 1988, 1993). The analysis of spectral matching and unmixing methods are used for many geological subjects and mineral mapping (e.g. Mustard and Pieters, 1986; Gillespie *et al.*, 1990; Boardman and Huntington, 1996; Staenz *et al.*, 1999; Neville *et al.*, 1998). The spectral mapping by using imaging spectroscopy data is a

common method in the remote sensing studies (Nolin and Dozier, 1993; Hamilton *et al.*, 1993). These studies showed that natural surfaces are rarely homogeneous. So spectral unmixing should identifies mixed endmembers and then evaluate their fractions (Plazel *et al.*, 2004). The umixing by using known endmembers is the most important method in the unmixing techniques (Boardman 1991; Boardman 1989) that has many applications in mineral and alteration mapping. Prihantarto *et al* (2012) have analyzed the soil features and mapped them based on mixing different

values of pixels and by using Earth Observing Advanced Land Imager (EO1-ALD) and unmixing methods. Van der Meer (2008) has classified minerals and provided their maps in south Spain by Landsat images based on unmixing methods. He used evaluated values of endmember spectrum and linear spectral mixing model. Staenz *et al* (2000) provided the map of minerals in Tundra and by using Constrain Linear Spectral Unmixing (CLSU) and Probe-1 airborne hyperspectral sensor provided detailed mineral mapping. Hosseinjani and Tangestani (2011) by using sub-pixel methods of LSU, Mixture Tuned Matched Filtering (MTMF) and ASTER images provided altered minerals and found that the MTMF method displays a higher accuracy in mineral mapping. Gabr *et al* (2010) by using the ASTER data and sub-pixel and N-dimensional feature space methods separate the hydrothermal alteration zones in west part of the Egyptian desert. Study of mineral mapping and soil characteristics based on unmixing methods have been done by many authors (e.g. Perry 2000; Kruse *et al.*, 2011; Kruse, 2012).

In this study we used hyperspectral images of EO-1 satellite and five unmixing methods for mineral and alteration mapping of two different areas (Mozahem volcano, Iran and Cuprite-Nevada, America) and compared their results.

2- Studied areas

The Mozahem volcano is located next to Shahr-e-Babak, Kerman province, SE Iran in the south part of Urumieh-Dokhtar volcanic belt. The selected area is on the volcano's caldera with longitudes of E $55^{\circ}12'00''$ - $55^{\circ}32'00''$ and latitudes of N $30^{\circ}13'00''$ till $30^{\circ}22'00''$. The Mozahem

volcano has Eocene igneous rocks that have been covered by lava, breccia and Neogene tuffs and its youngest sediment unit consists of sandstone and Neogene conglomerate.

The Cuprite in Nevada, USA has with longitudes of W $117^{\circ}9'00''$ – $117^{\circ}13'00''$ and latitudes of N $37^{\circ}30'00''$ – $37^{\circ}34'00''$. Because of spread individual lithological units, this area is very ideal for remote sensing studies (Rowan *et al.*, 2003; Clark *et al.*, 2003; Swayze *et al.*, 2003; Mars and Rowan, 2006; Kruse, 2012 among others). These studies indicated that the Cuprite area shows high mineralization of hematite, jarosite, goethite, muscovite, chlorite, calcite (Fig. 1).

3- Methodology

3.1- Preprocessing

Hyperion images have several errors that it is necessary to correct them before use that for analysis. So some modification was implemented as below. Based on metadata file on level 1R images, some processing steps such as the correction of Echo, Smear, and Dark object subtraction have been done. According to analyzing images of these zones, bad bands were omitted (84 bands of Mozahem volcano and 77 bands of Cuprite area) and based on determined values (Barry 2001) by scaling factor, converting DN to radiance by dividing in two parts SWIR and VNIR has been done. Then by a set of data and level 1R images bad pixels have been omitted. To remove streaks of images, the Datt *et al*'s (2003) method was used. Analyzing MNF-1 images in SWIR and VNIR showed us there is a gradient in grey levels in VNIR. To do so column mean adjusted in MNF space that was used by Goodenough *et al* (2003) for Hyperion images, was used for

smile correction. Then Internal Average Reflectance (IAR) method was used to reduce the atmosphere effects that are applied for desert areas (Kurse 1988, Robert 1986, Ben-Dor *et al* 1994). For geometric correction with some problems in SWIR by using GPS points and suitable diffusion, conformity of VNIR and SWIR was modified.

3.2- Classification of Minerals and alterations

Before classifying the images, due to the high noise and number of spectral bands, the MNF (Green, *et al.*, 1988) transformation was performed on the

datasets. In other words, in a common practice, MNF components with eigenvalues less than one are usually excluded from the data as noise in order to improve the subsequent spectral processing results (Research Systems Inc., 2003). Since the eigenvalues of 15 MNF images of the data were greater than one, the 15 bands were retained for subsequent data processing in two study areas. This step is a statistical data reduction technique that performs a series of two Principal Components Analyses (PCA) to isolate noise and reduce the dimensionality of a hyperspectral dataset (Green *et al.*, 1988).

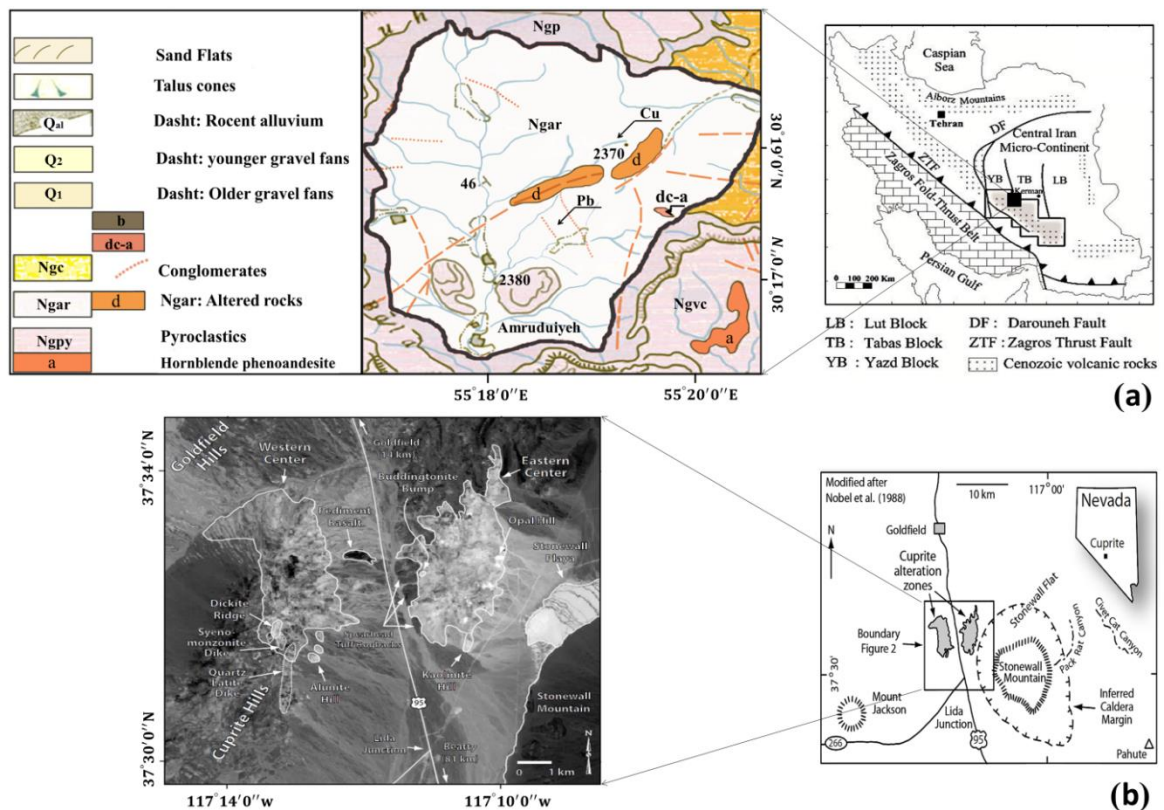


Figure 1a) Mozaheh volcanic, Iran, b) Cuprite Nevada (Swayze *et al.*, 2010).

In this study, to examine the classification of geological units of the five general methods used which have different structural functions. These functions divided in three basic concepts. The first used method was Spectral Angle Mapper (SAM) that uses the angular difference

between observation vector and source spectrum in spectral space to determine the possible percent of target existence. In the classification by using this method, it is assumed that data is in reflection stage and mistakes are not considerable (Kurse and Lefkoff, 1993). But the second and third

methods have linear base structure. An important assumption of LSU is that the reflectance at each pixel of the image is the linear proportion-weighted combination of the reflectance of each endmember present within the pixel (Smith *et al.*, 1990). Orthogonal Subspace Projection (OSP) is an unconstrained and another linear based method that only can detect one target in each implementation. It removed undesired targets and tries to improve the result of detection. Indeed, it does it by breaking matrix to desired target vector and undesired target (Mangari *et al.*, 2010). The concept of this operator is the production of orthogonal subspace on undesired target spectral vectors. If the undesired target spectral vectors brought into such a subspace, they would be removed because the image of a vector on orthogonal subspace is equal to zero. If spectral vector of a desired pixel is projected in such a space, the similarity of the pixel with the target or lack of similarity with the background may be observed.

One of the OSP method constrains is its needs to some information about characterizations of undesired spectral target, which is very difficult to get this information. But for the whole extraction of such information we should estimate some undesired targets in the image. Totally, Constrained Energy Minimization (CEM) is a semi-supervised method and uses FIR filter, which passes the received energy in one direction and minimizes received energy of other sources (Chang, 2003). Adaptive Coherence Estimator (ACE) is another covariance based method that uses a distribution function for modeling background. In other words, this method does not need to use spectrum of pure parts of background that is equal to removing

structural background. In this method background is considered as a Gaussian distribution function that the average is zero and covariance is $\sigma^2 \Sigma$. Therefore, these five methods that are shown in the Table 1 were used to mapping the alterations and lithological units in two study areas.

4- Results

In order to compare and evaluate of lithological mapping methods with dominant mineral and alteration zones, the following methods are used: Confusion matrix, computing Kappa coefficient and analyzing the amount of the separability of classes by using Jeffries-Matusita index (Bhattacharyya, 1943). The used data are gathered by field studies and previous reports. As the Figure 2a and 2b show, the LSU results are better for separation of lithological units by dominant mineral in comparison with the others and it has 19.89 percent more accurate than the second rank method (i.e. ACE). However, for alteration mapping the ACE method shows the best results and its overall accuracy and Kappa coefficient are 69.54% and 0.5448, respectively, while the LSU method acquires third rank. The result of classes discrimination by using Jeffries-Matusita index in Cuprite area shows that the LSU method has high accuracy (e.g. 0.949) rather than other methods (Fig. 3). The results of this index for Mozahem volcano are close to the result of Cuprite area (Figure 4). The results of SAM in Mozahem volcano have low accuracy in spite of its high ability for class discrimination. This is could be caused by false classification of highly and weakly altered units. In other words, although the altered units have easily separated from

together but this method by using weakly altered unites and causes the mistake. altered units samples, classified high

Table 1) The used methods for this study, where d is the target spectrum, x is the pixel spectrum, f is proportions of the various endmembers in a pixel, Σ is covariance matrix and R is the background correlation or covariance matrix.

	Target detection method	Target detection function	Reference
Angular base	Spectral Angel Mapper (SAM)	$T_{SAM} = \frac{d^T x}{(d^T d)^{1/2}(x^T x)^{1/2}}$	kurse and Lefkoff, 1993
Covariance base	Adaptive Coherence Estimator (ACE)	$T_{ACE} = \frac{(d^T \Sigma^{-1} x)^2}{(d^T \Sigma^{-1} d)(x^T \Sigma^{-1} x)}$	Kraut et al., 2005
	Constrained Energy Minimization (CEM)	$T_{CEM} = \frac{R_{L \times L}^{-1} d}{d^T R_{L \times L}^{-1} d} x$	Farrand and Harsanyi, 1994
Linear base	Orthogonal Subspace Projection (OSP)	$T_{OSP} = \frac{d^T P_{\bar{v}} x}{d^T P_{\bar{v}} d}$	Chang, 1998
	Linear Spectral Unmixing (LSU)	$f = (A^t A)^{-1} A^t x$	Boardman, 1989

The SAM method shows low accuracy for alteration classification of Mozahem volcano. It is because of the same direction occurring of base and target vectors with different values. In this condition, because of computing of vector length the both pixels acquire the same value, while actually they are different, especially when the spectral signatures of training samples come closer to each other. Because the source of these two methods is MNF transformation, the analysis of spectral signature can describe it better (Figure 5).

As shown in Figure 5a the pixel values of the first MNFs in Mozahem volcano show small difference with those of Cuprite. This closeness in spectral values of MNF in

Mozahem volcano takes place in the first bands of spectral values in MNF, while in Cuprite it starts from sixth band the spectral difference of training samples remains constant and enlarges the angle of spectral difference, reference and target spectrum, that improve the efficiency of the SAM in Cuprite area compared with Mozahem volcano.

The ACE and the CEM are based on image covariance, however in some cases the matrix of covariance has been used. The disadvantage of these methods is that the matrix of covariance is produced only once for all pixels, and surrender of the pixel values it is constant which could reduce accuracy of detection.

If the pixel values have high differences the CEM and the ACE methods, an overall covariance cannot be a suitable weight for all pixels. Because of high spectral difference in MNF space (Figure 5a) in

Cuprite in compared with Mozahem volcano (Figure 5b) it is expected that these two methods is suitable for the Mozahem volcano, because its low spectral differences of training samples (Fig. 5).

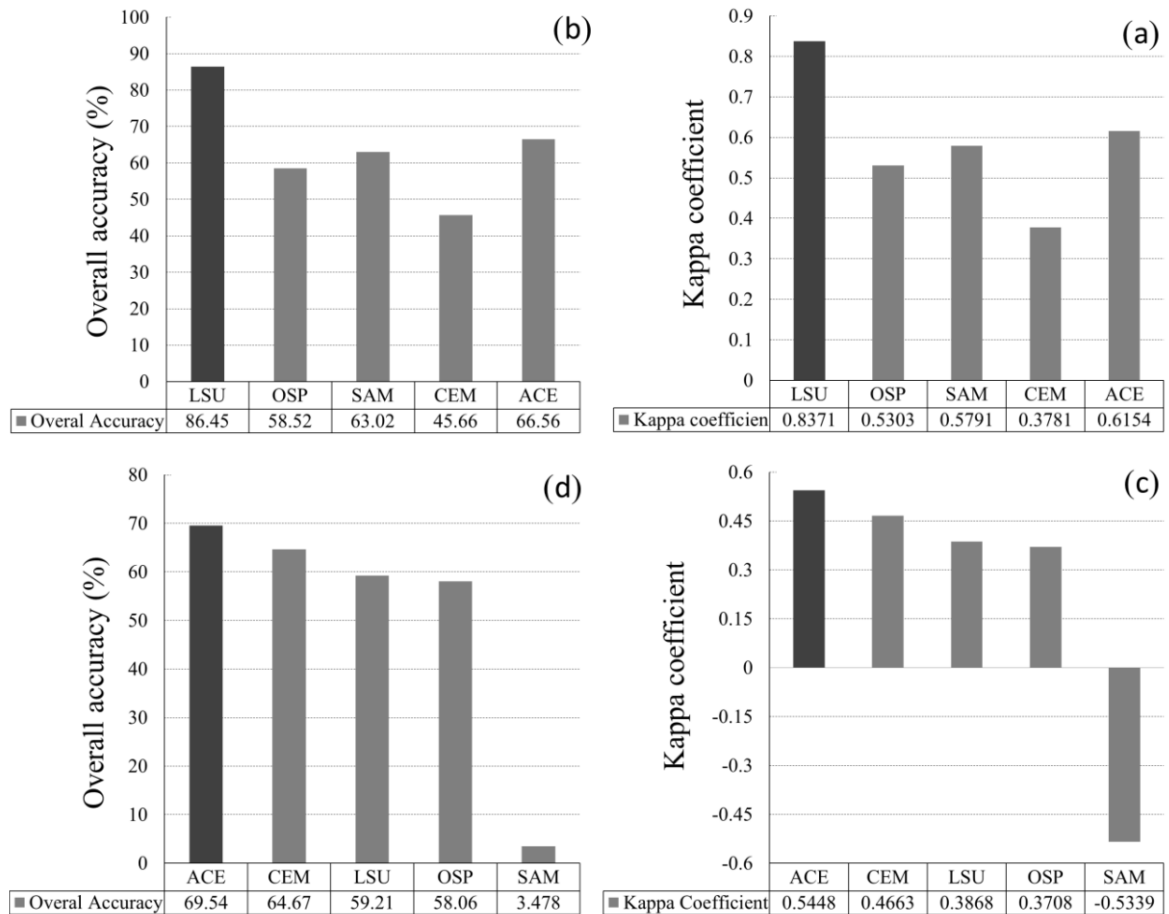


Figure 2) The Kappa coefficient and confusion matrix values of the study areas. a) Kappa coefficient for cuprite area; b) The confusion matrix for Cuprite area; c) Kappa coefficient for Mozahem volcano; d) The confusion matrix Mozahem volcano.

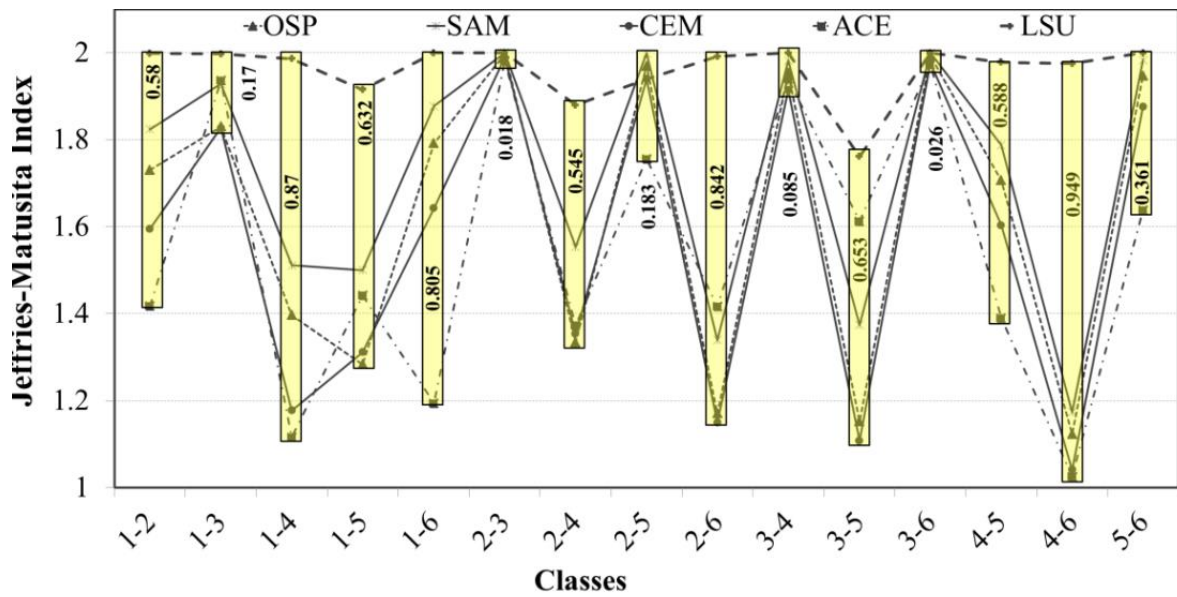


Figure 3) The results of Jeffries-Matusita index in output image of detectors in the Cuprite area (rectangles show the low and high changes in the values of this index in each pair class).

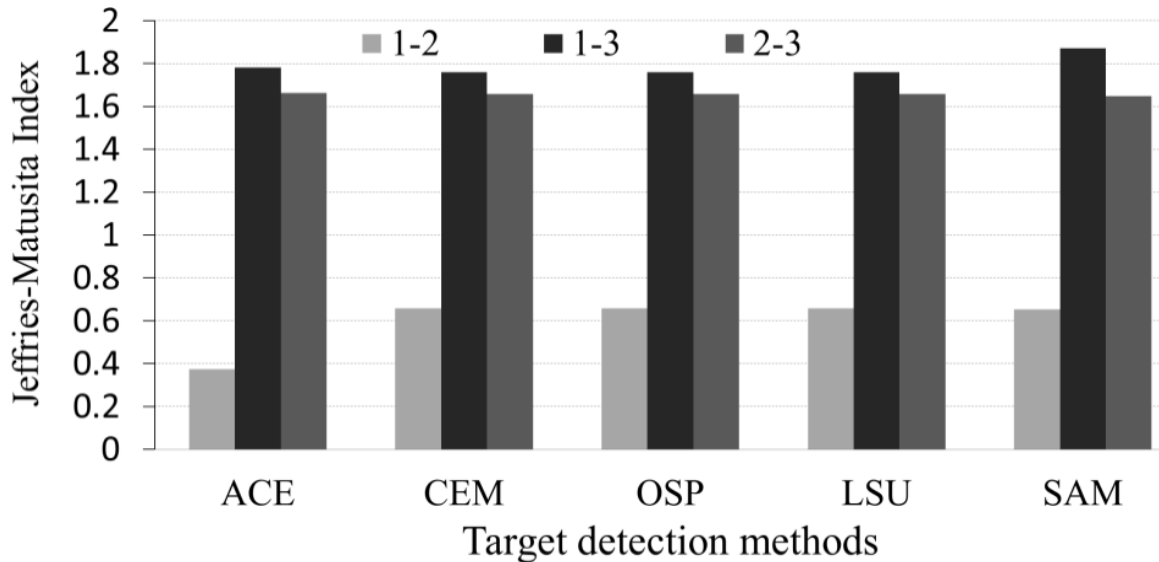


Figure 4) The Jeffries-Matusita indexes for output image of detectors on three classes for the Mozahem volcano.

In these cases linear evaluation methods such as OSP and LSU act well and in the studied area the LSU shows good results. In OSP because of the presence of orthogonal subspace and separation of target matrix into matrix of desired and undesired types, in each stage they show different results in compared with LSU. This separation is to

improve the accuracy but the presence of spectrum of non-target can be considered as a noise, which decreases the accuracy in compared with LSU. Figures 6 and 7 show the classified image of each method based on overlaying of the Hyperion detector images.

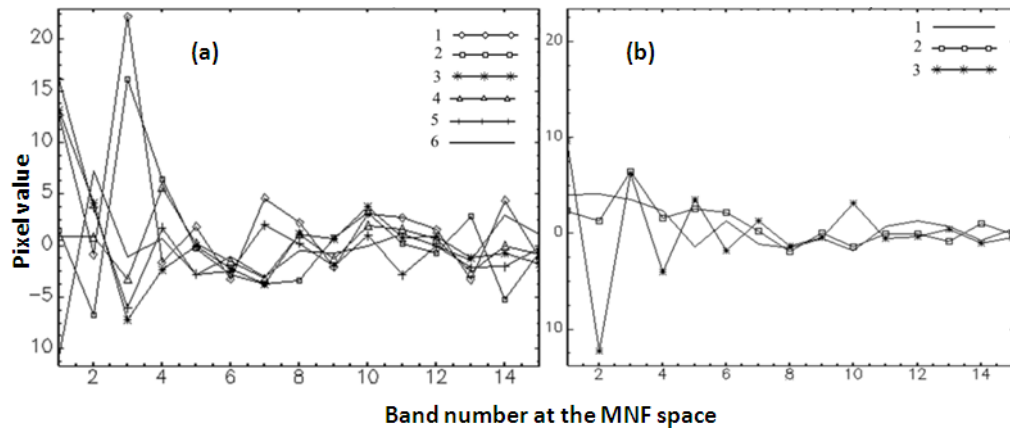


Figure 5a) The average spectral signature of training samples for each class in the first fifteen bands of MNF in Cuprite area (1) Jarosite+Geothite; 2) Hematite; 3) Chlorite + Muscovite; 4) Alluvial fan; 5) Fe-bearing minerals +Muscovite; 6) Fe-bearing minerals; b) The average spectral signature of training samples for each class in the first fifteen bands of MNF for three alteration units in Mozahem volcano (1) Low altered andesites -pyroclastic rocks; 2) Andesites and granodiorite with medium alteration-phyllitic alteration; 3) High altered clays and serisite -argillic alteration.

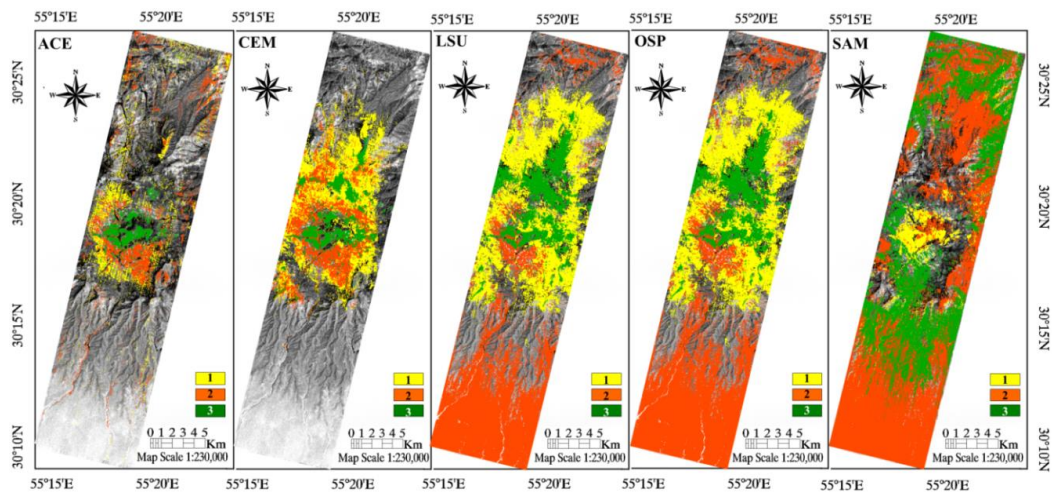


Figure 6) The classification of three alteration units in the Mozahem volcano in Shar-e-Babak based on five used methods that overlaying on 8th band of Hyperion image.

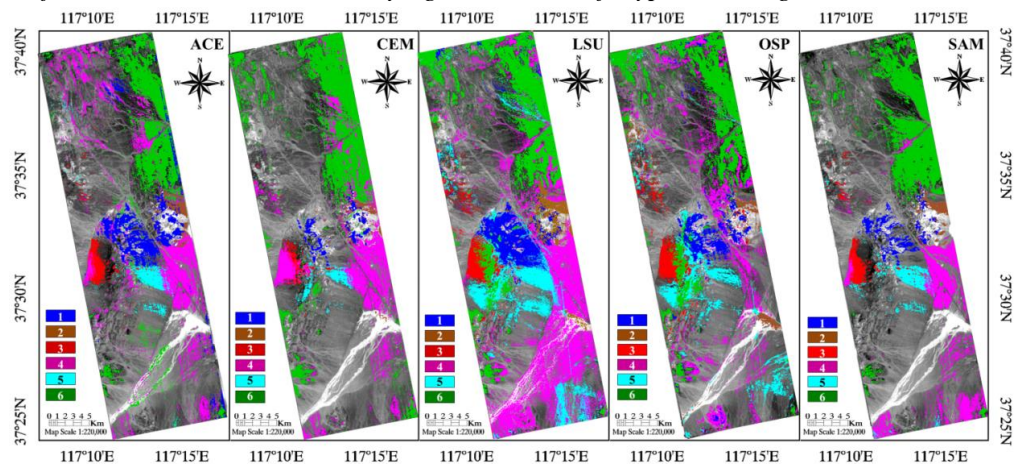


Figure 7) The classification of six units in the Cuprite-Nevada based on five used methods that overlaying on 8th band of Hyperion image.

5- Conclusions

The analyzing of target detection in a sub-pixel level shows that the methods are highly depend on the difference between spectral signatures of source samples and in covariance methods of ACE and CEM the change of covariance matrix could affect the accuracy. In the linear methods such as LSU and OSP, this spectral signature differences is less effective. The highest changes in results took place for the SAM method. As a whole, the results show that sub-pixel methods of LSU, OSP, CEM, and SAM are more effective for separation of lithological units with dominant mineral than alteration classification and the Hyperion images can provide accurate maps.

References

- Bhattacharyya, A.A. 1943. On a measure of divergence between two statistical populations defined by their probability distributions. *Bulletin of the Calcutta Mathematical Society*: 35, 99–110.
- Boardman, J.W. 1989. Inversion of imaging spectrometry data using singular value decomposition. in *Proc. IEEE Symp. Geoscience and Remote Sensing*: 2069–2072.
- Boardman, J.W. 1991. Sedimentary facies analysis using imaging spectrometry: A geophysical inverse problem. Unpublished Ph.D. dissertation, Univ. Colorado, Boulder, CO, 212 p.
- Boardman, J.W., Huntington, J.H. 1996. Mineral mapping with 1995 AVIRIS data: in *Summaries of the 6th Annual JPL Airborne Earth Science Workshop*, JPL Pub. 96-4, Vol. 1. AVIRIS Workshop, Jet Propulsion Laboratory, California Institute of Technology, Pasadena, Calif., p. 9–11.
- Chang, C.I. 1998. Further results on relationship between spectral unmixing and subspace projection. *IEEE Transactions on Geoscience and Remote Sensing*: 36, 1030–1032.
- Chang, C.I. 2003. *Hyperspectral Imaging techniques for spectral detection and classification*. Orlando Kluwer Academic.
- Clark, R.N., Swayze, G.A., Livo, K.E., Kokaly, R.F., Kokaly, S.J., Dalton, J. B., McDougal, R.R., Gent, C. A. 2003. Imaging spectroscopy: Earth and planetary remote sensing with the USGS Tetracorder and expert systems. *The Journal of Geophysical Research*: 108, 5–44.
- Farrand, W.H., Harsanyi, J.C. 1994. Mapping distributed geological and botanical targets through constrained energy minimization. *Proceedings, 10th Thematic Conference on Geological Remote Sensing*, San Antonio, TX, 9–12, I-419–I-429.
- Gabr, S., Ghulam A., Kusky T. 2010. Detecting areas of high-potential gold mineralization using ASTER data. *Ore Geology Reviews*: 38, 59–69.
- Gillespie, A.R., Smith, M.O., Adams, J.B., Willies, S.C., Fischer, A.F., Sabol, D.E. 1990. Interpretation of Residual Images: Spectral Mixture Analysis of AVIRIS Images, Owens Valley, California. *Proceedings of the Second Airborne Visible/Infrared Imaging Spectrometer (AVIRIS) Workshop*, Pasadena, CA, JPL Publication: 90–54, 243–270.

- Green, A.A., Berman, M., Switzer, P., Craig, M.D., 1988. A transformation for ordering multispectral data in terms of image quality with implications for noise removal. *IEEE Transactions on Geoscience and Remote Sensing*: 26, 65–74.
- Hamilton, M.K., Davis, C.O., Rhea, W.J., Pilorz, S.H., Carder, K.L. 1993. Estimating chlorophyll content and bathymetry of Lake Tahoe using AVIRIS data: *Remote Sensing of Environment*: 44, 217–230.
- Hosseinjani, M., Tangestani, M. H. 2011. Mapping alteration minerals using sub-pixel unmixing of ASTER data in the Sarduiyeh area SE Kerman, Iran. *International Journal of Digital Earth*: 4, 487–504.
- Kraut, S., Scharf, L.L., Butler, R.W. 2005. The Adaptive Coherence Estimator: A Uniformly Most-Powerful-Invariant Adaptive Detection Statistic. *IEEE Transactions On Signal Processing*, vol. 53, 427-438.
- Kruse, F.A. 2012. Mapping surface mineralogy using imaging spectrometry, *Geomorphology*: 137, 41–56.
- Kruse, F.A., Lefkoff, A.B. 1993. Knowledge-based geologic mapping with imaging spectrometers. *Remote Sensing Reviews*: 8, 3–28.
- Kruse, F.A., James, V., Taranik, M.C., Joshua, M., Elizabeth, F., Littlefield, W., Calvin, M., Brigitte, A.M. 2011. Effect of Reduced Spatial Resolution on Mineral Mapping Using Imaging Spectrometry Examples Using Hyperspectral Infrared Imager (HypIRI)-Simulated Data. *Remote Sensing*: 3, 1584–1602.
- Mangari, U.G., Samanta, S., Das, S., Chowdhury, P.R. 2010. A survey of decision fusion and feature fusion strategies for pattern classification. *IEEE Technical review*: 27, 293–307.
- Mars, J.C., Rowan, L.C. 2006. Regional mapping of phyllic- and argillic-altered rocks in the Zagros magmatic arc, Iran, using Advanced Spaceborne Thermal Emission and Reflection Radiometer (ASTER) data and logical operator algorithms. *Geosphere*: 2, 161–186.
- Mustard, J.F., Pieters, C.M. 1986. Abundance and Distribution on Mineral Components Associated with Moses Rock (Kimberlite) Diatreme. *Proceedings of the Second Airborne Imaging Spectrometer Data Analysis Workshop, Pasadena, CA, JPL Publication*: 86–35, 81–85.
- Neville, R.A., Nadeau, C., Levesque, J., Szeredi, T., Staenz, K., Hauff, P., Borstad, G.A. 1998. Hyperspectral Imagery for Mineral Exploration: Comparison of Data from Two Airborne Sensors. *Proceedings of the International SPIE Symposium on Imaging Spectrometry, San Diego, CA. Society of Photo-Optical Instrumentation Engineers*: 3438, 74–82.
- Nolin, A.W., Dozier, J. 1993. Estimating snow grain size using AVIRIS data. *Remote Sensing of Environment*: 44, 231–238.
- Prihantarto, W. A., Nugroho, Y. A., Wicaksono, P., Barianto, B. H. 2012. Soil prime minerals mapping using linear spectral unmixing technique in multispectral imagery data. *Japan Geoscience Union Meeting, May 20-25, Makuhari, Chiba, Japan*, p.1.

- Research Systems Inc. 2003. ENVI Tutorial, ENVI Software Package Version 4.0.
- Rowan, L., Hook, S., Abrams, M., Mars, J. 2003. Mapping hydrothermally altered rocks at Cuprite, Nevada using the Advanced Spaceborne Thermal Emission and Reflectance Radiometer (ASTER), a new satellite imaging system. *Economic Geology*: 98, 1019–1027.
- Smith, M.O., Ustin, S.L., Adamsa, J.B., Gillespie, A.R. 1990. Vegetation in deserts: I. A regional measure of abundance from multispectral images. *Remote Sensing of Environment*: 31, 1–26.
- Staez, K., Nadeau, C., Secker, J., and Budkewitsch, P. 2000. Spectral Unmixing Applied to Vegetated Environments in the Canadian Arctic for Mineral Mapping. XIXth ISPRS Congress and Exhibition, Amsterdam, July 15–23.
- Staez, K., Neville, R.A., Levesque, J., Szeredi, T., Singhroy, V., Borstad, G.A., Hauff, P. 1999. Evaluation of CASI and SFSI Hyperspectral Data for Environmental and Geological Applications: Two Case Studies. *Canadian Journal of Remote Sensing*: 25, 311–322.
- Swayze, G.A., Clark, R.N., Goetz, A.F.H., Chrien, T.G., Gorelick, N.S. 2003. Effects of spectrometer band pass, sampling, and signal-to-noise ratio on spectral identification using the Tetracorder algorithm. *Journal of Geophysical Research*: 108, 5105.
- Swayze, L.W., Livo, K.E, Lowers, H.A., Ashley, R.P., and Kruse, F.A. 2010, Mapping Advanced Argillic Alteration at Cuprite, Nevada Using Imaging Spectroscopy. U.S. Geological Survey publication: Pp 1–90.
- Van der Meer, F. 2008. Mineral mapping and landsat thematic mapper image classification using spectral unmixing. *Geocarto International*: 12, 27–40.
- Vane, F.H.G., Solomon, J.E., Rock, B.N. 1985. Imaging spectrometry for Earth remote sensing. *Science*: 228, 1147–1153.
- Vane, G., Goetz, A.F.H. 1988. Terrestrial imaging spectroscopy. *Remote Sensing of Environment*: 24, 1–29.
- Vane, G., Goetz, A.F.H. 1993. Terrestrial imaging spectrometry: current status, future trends, *Remote Sensing of Environment*: 44, 117–126.